Rev.Adv.Mater.Sci. 5 (2003) 57-61

GROWTH AND MORPHOLOGY OF LOW-ENERGY DEPOSITED Cu NANOCLUSTER FILMS

G. Palasantzas, S. A. Koch and J. Th. M. De Hosson

Department of Applied Physics, Materials Science Centre and Netherlands Institute for Metals Research, University of Groningen, Nijenborgh 4, 9747 AG Groningen, The Netherlands

Received: June 21, 2003

Abstract. Growth front aspects of copper nanocluster films deposited with low energy onto silicon substrates at room temperature are investigated using atomic force microscopy. Analyses of the height-difference correlation function yield a roughness exponent H=0.45±0.05. The rms roughness amplitude w evolves with deposition time as a power law, $w \propto t^{\beta}$, with a growth exponent β=0.62±0.07. These scaling exponents, in combination with an asymmetrical height distribution, suggest a complex non-linear roughening mechanism dominated by the formation of pores, resulting in a low density film. X-ray scattering reflectivity measurements indicated pore sizes as low as 5 nm.

1. INTRODUCTION

Direct deposition of atomic clusters to grow thin films has attracted considerable interest, both from a fundamental and an application point of view [1, 2]. This method offers flexibility because the clusters are preformed in the gas phase; the effects of nucleation and growth on a specific substrate are avoided. The properties of the building block (size, kinetic energy) can be carefully controlled leading to an interesting range of possible film structures [1]. Several investigations of the surface morphology of cluster-assembled films have indicated the presence of self-affine surface roughness [3, 4]. By characterizing the surface roughness evolution, it is possible to extract quantitative relations between roughness and film thickness [5]. The roughness exponent H quantifies the degree of surface irregularity at short length scales, while the growth exponent β describes how the interface width evolves with time [5].

For high-energy Cu cluster beams it has been shown [3] that the growth mode can be described by the Edwards-Wilkinson (EW) equation $\partial h/\partial t = \gamma\nabla^2 h+\eta$, with h the surface height, η a random deposition noise, and γ a surface relaxation coefficient [6]. The EW equation corresponds to the case of random deposition with surface relaxation [6]. It yields a roughness exponent H=0 in 2+1 dimensions, which is characteristic of logarithmic roughness, i.e. the correlation function is proportional to log(r) at short lengths r [5, 7]. Similarly, the growth exponent is β=0 yielding a logarithmic growth of the rms roughness amplitude with deposition time. On the other hand, growth studies of carbon nanocluster films deposited at low energy (below 0.5 eV per atom) onto Si and polycrystalline Cu substrates, revealed roughness exponents in the range H=0.64-0.68 and growth exponents β=0.42-0.50 [7]. These values did not significantly depend on the average cluster size, although the growth of the films was affected by the presence of relatively large particles in the beam causing local morphology fluctuations [7].

In the present work we investigate Cu nanoclusters with a narrow size distribution, deposited at low energy to make cluster-assembled films. The metallic nature of these particles means that local cluster coalescence is more likely to occur

Corresponding author: G. Palasantzas, e-mail: g.palasantzas@phys.rug.nl

than for carbon, where covalent bonding effectively prohibits such processes. The time evolution of surface morphology and roughness of such films is analyzed quantitatively using atomic force microscopy (AFM). Furthermore, the internal film structure is discussed using results from transmission electron microscopy (TEM) and X-ray reflectivity.

2. EXPERIMENTAL PROCEDURE

Clusters were formed with the gas aggregation technique, using a DC magnetron-equipped deposition source from Oxford Applied Research [1]. The base pressure in the deposition chamber was ~10^{-8} mbar. During magnetron sputtering with Ar gas the pressure was typically ~10^{-4} mbar. The power for sputtering was ≈ 60 Watts (300 V and plasma current 0.2 A). A series of films was prepared with deposition times ranging from 5 s to 25 min. The average deposition rate was ≈ 4.5 nm/min, a value obtained from Auger depth profile analysis to determine film thickness. Substrates were either pieces of single crystalline Si(100), or thin foils of Si_3N_4 with 50 nm thickness for the purpose of transmission electron microscopy (TEM).

The film surface morphology was examined using an AFM (Digital Instruments Dimension 3100) in tapping mode to avoid any damage of the film surface. The AFM tip and cantilever are an integrated assembly of single crystal silicon produced by etching techniques, with a tip radius ≤ 10 nm and tip side angle ≤ 10°. For each value of the film thickness, the height-difference correlation function $g(x)=\langle[h(x)-h(0)]^2\rangle$ was computed in the fast scan direction, where $h(x)$ is the surface height at lateral position 'x' relative to the mean height. Averages were taken over five images acquired at different positions on the sample, each image consisting of 512x512 pixels. In general, for a self-affine rough morphology we have $g(x)=\rho^2 x^{2H}$ for $x<<\xi$ and $g(x)=2w^2$ for $x>>\xi$ [5,8,9]. In these relations ρ represents the average local surface slope, ξ the lateral correlation length and w the rms roughness amplitude. In a double-log plot the saturation regime of $g(x)$ yields w, and the roughness exponent H is calculated from the slope of $g(x)$ at small lengths x. Finally, the correlation length x is given by $\xi=(2w^2/\rho^2)^{1/2H}$, from the intersection of the power-law and saturation lines.

3. RESULTS

3a. Microscopy analysis

Upon short deposition to a coverage below the percolation threshold, a random distribution of clusters was observed on either Si or Si_3N_4 (Fig. 1, left inset). There is no evidence of surface diffusion of entire clusters. Larger clusters are only formed due to coalescence processes after direct impact on a previously deposited cluster. This is reflected in the cluster size distribution shown in Fig. 1, which has a smaller peak next to the main peak and can be adequately represented by a double Gaussian curve. TEM analysis indicated a supported cluster diameter of approximately 10 nm, as well as the presence of different crystallographic orientations within the same cluster (Fig. 1, right inset). Furthermore, in AFM images a rim around the clusters is oberved indicating a partial submergence into the substrate, so that clusters are partly covered by substrate material [10]. This can be explained by the fact that the surface energy of Cu, γ_{Cu}=1.75 J/m^2, is somewhat larger than that of Si, γ_{Cu}=1.4 J/m^2 [11]. Submergence is driven by large capillary forces on the cluster particles. It can occur in all systems if the nanoparticle has sufficient kinetic energy and a higher surface energy than the substrate. In the opposite case the particle would simply wet the substrate [12].

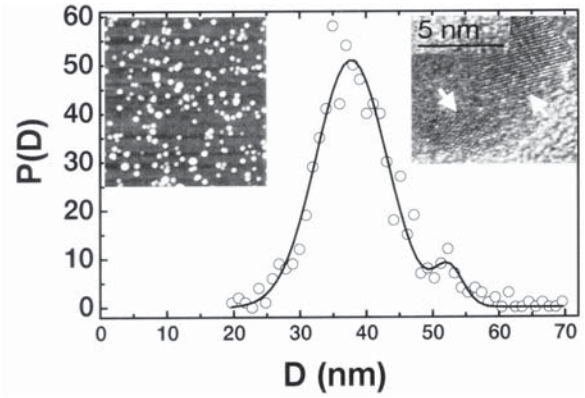

Fig. 1. Cluster diameter distribution determined from AFM images, where the fit (solid line) is a double Gaussian distribution with widths w_{1D}=7.9 nm and w_{2D}=28.5 nm. The left inset shows a 1x1 мm^2 AFM image of a random distribution of clusters on Si. The right inset shows a high-resolution TEM image of a single Cu cluster, where arrows indicate different crystallographic orientations.

For closed (continuous) films the measured height distribution showed deviations from a Gaussian shape. To quantify this point further we calculated the skewness S, which is a measure of the distribution symmetry around a reference surface level. For

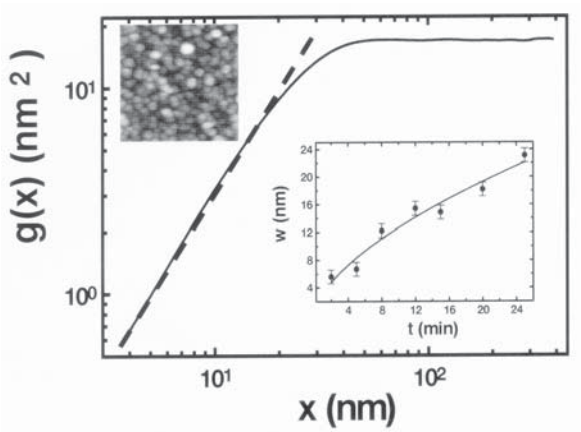

Fig. 2. Correlation function $g(x)$ vs lateral scale x, for images of scan size 2 μm. The linear fit yields the exponent H=0.49±0.03, and the saturation regime w=6.7 nm. For the correlation length we obtain ξ=31 nm which is comparable to cluster sizes shown in the AFM image (left inset, scan size 500 nm). The right inset shows rms amplitude w vs. deposition time t.

a Gaussian distribution S=0, while in the present case we obtained for each film thickness S>0, indicating breaking of the $h \rightarrow -h$ symmetry. This is possibly related to the presence of a non-linearity associated with dependence of growth on the local surface inclination [10, 13]. Furthermore, the growth of out-of-plane correlations (rms amplitude w) is quantified by the growth exponent β such that $w \propto t^{\beta}$ [8, 10] where measurement yields β=0.62±0.07 (Fig. 2, right inset). Measurements of the roughness exponents H yielded H=0.45 ± 0.05 for all closed films.

The measured exponents H might be slightly overestimated due to the influence of the finite AFM tip radius [14]. At any rate, especially for later stages of growth they are close to the value predicted by the KPZ (Kardar-Parisi-Zhang) model [13]. In this model the dominant relaxation mechanisms are desorption or vacancy formation, with a roughness exponent $H_{KPZ} \approx 0.4$ [13]. In our case vacancy formation is a result of the soft landing of the Cu clusters, resulting in a porous film [1]. However, deviations from a pure KPZ type of growth are introduced by cluster coalescence processes driven by local atomic diffusion. In addition, there is still a possible influence from quenched disorder [4]. This might explain that the growth exponent β is larger than that of the KPZ scenario ($\beta_{KPZ} \approx 0.25$).

Surface diffusion of deposited clusters would lead to a characteristic roughness exponent H>0.6 [15]. Moreover, during the early deposition stages the cluster diffusion coefficient scales with size or number of atoms within the cluster 'n' as $D_n = D_1/n^c$ (c>0) [3, 16], leading to very small coefficients ($D_n << D_1$) for clusters of size 10 nm. In fact, since c=0.3-1.7 [16] and $n \approx 3.6 \cdot 10^5$ (for a spherical cluster of diameter 10 nm); we will have in the case of c=0.3, $D_n/D_1 \sim 0.03$. Therefore, surface diffusion of entire Cu clusters can be largely excluded as an important surface relaxation mechanism.

3b. X-ray analysis

X-ray reflectivity measurements were performed with a wavelength of λ=0.154 nm and in geometries for both specular and off-specular (diffuse) scattering; the results are shown in Fig. 3. Since the film used for analysis was relatively thick (d >100 nm) on a very smooth substrate (rms roughness amplitude ~0.3 nm), contributions to the scattered intensity from the Cu/Si interface were ignored. The specularly scattered x-ray intensity is recorded as a function of the wave vector transfer q which is the difference between the scattered and incident wave vectors. When θ is the incident angle measured from the sample surface then $q_z = (4\pi/\lambda)\sin\theta$. From Fig. 3, the angle of total external reflection corresponds to a wave vector $q_z \approx 0.35$ nm^{-1}. At the same time we have from Snellius' law $\cos\theta_c = n$, with n the refractive index. Neglecting the absorption term in n, $n = 1 - r_e \langle\rho\rangle \lambda^2/2\pi$, with $r_e = 2.8 \times 10^{-6}$ nm the classical electron radius and $\langle\rho\rangle$ the average electron density of the material. From this we obtain an average electron density $\langle\rho\rangle \approx 0.5\rho_{bulk}$ which is significantly lower than the bulk density in agreement with the porous film structure.

Furthermore, the specular component (Fig. 3) at large q_z ($q_z w$>1) falls off with a power-law $I_{specu} \propto q_z^{-(4.43\pm0.02)}$ instead of a pure $I_{specu} \propto q_z^{-4}$ characteristic of a smooth surface. If however, we consider the scattering from porous scatterers, in which the pore boundaries can be described in terms of a fractal dimension D [17], then the scattered intensity should vary with q_z as $I(q_z) \propto q_z^{-(7-D)}$ (taking into account that the area illuminated by the X-ray beam varies as $\propto q_z^{-1}$). The latter yields with 7-D=4.43 a fractal dimension D=2.57 which is typical for porous systems [17]. In addition, a rough estimate of the pore size R_{pore} can be performed by the smallest value of $q_{z,min}$ [18] after which the power law for $I(q_z)$ is observed, based on the relation $q_{z,min} R_{pore} \approx 5$ ($q_{z,min} R_{pore} >> 1$) [18]. Since $q_{z,min} \approx 1$ nm^{-1} it is expected that $R_{pore} \approx 5$ nm or larger.

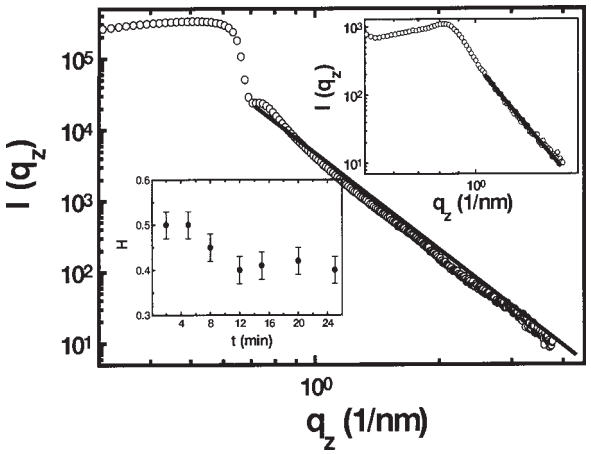

Fig. 3. Specular reflectivity vs. wave vector transfer along the *z*-direction (out of the film plane). The upper inset shows off-specular reflectivity measurements. The solid lines are guides for the eye to show where the power-law behavior appears. The lower inset shows the variation of the roughness exponent *H* with deposition time.

Finally, we proceed with the analysis of the diffuse off-specular scattered intensity (Fig. 3, inset) measured at an angle 0.05° out of the specular condition (detector was at angle θ-0.05° from the incidence angle θ). At large q_z(q_zw>1) the scattered intensity fall with an inverse power-law behavior $I_{dif}(q_z) \propto q_z^{-(5.75\pm0.1)}$. On the other hand the single layer reflectivity under these conditions is known to follow the power-law decrement $I_{dif}(q_z) \propto q_z^{-(3+1/H)}$ [17, 19, 20]. The latter yields a roughness exponent H=0.37 which is close to the ones measured by AFM, taking into account that tip size effects may result in higher measured values [14].

4. CONCLUSIONS

In conclusion, we have investigated growth front aspects of Cu nanocluster films deposited onto silicon substrates at room temperature. The asymmetrical height distribution (breaking of $h \rightarrow -h$ symmetry) together with the measured scaling exponents suggest a complex non-linear roughening mechanism, dominated by vacancy formation and leading to porous films. Pore sizes are ≥ 5 nm as X-ray reflectivity measurements indicate.

Notably, the random deposition process ($w \propto t^{1/2}$) provides an upper bound for the value of the roughness exponent β=1/2 which is attained if every particle remains on the height level where it was deposited, while any surface relaxation leads to values β<0.5. Roughness beyond the random deposition can occur only if matter is transported to higher layers, which would require a thermodynamic driving force, as, e.g., in dewetting. However, such a thermodynamic instability is not present for the Cu cluster films. Rapid roughening with β>0.5 has been reported for a number of systems [20], but no general mechanism has been identified. Nevertheless, it is plausible that, when certain regions of the surface persistently grow faster than others, the surface will roughen rapidly.

ACKNOWLEDGEMENTS

We would like to acknowledge financial support from the MSC^{plus} program. We thank T. Vystavel for TEM analysis, and T. Hibma for X-ray reflectivity measurements.

REFERENCES

[1] H. Haberland, M. Moseler, Y. Qiang, O. Rattunde, T. Reiners and Y. Thurner // *Surf. Review and Lett*. **3** (1996) 887; H. Haberland, M. Karrais, M. Mall and Y. Thurner // *J. Vac. Sci. Technol. A* **10** (1992) 3266. For details on our deposition system see http://www.oaresearch.co.uk/cluster.htm.

[2] P. Jensen // *Rev. Mod. Phys.* **71** (1999) 1695.

[3] M. Moseler, O. Rattunde, J. Nordiek and H. Haberland // *Nuclear Instruments and Methods in Physics Research B* **164-165** (2000) 522.

[4] R. Buzio, E. Gnecco, C. Boragno, U. Valbusa, P. Piseri, E. Barborini and P. Milani // *Surf. Sci.* **444** (2000) L1.

[5] Y. P. Zhao, G. -C. Wang, T. -M. Lu, *Characterization of amorphous and crystalline rough surfaces - Principles and applications* (Experimental Methods in the Physical Science Vol. 37, Academic Press, 2000).

[6] S. F. Edwards and D. R. Wilkinson // *Proc. R. Soc. Lond. A* **381** (1982) 17.

[7] See ref. 5 for analytic solution of the EW model. Moreover, from power-law we can obtain logarithmic behaviour if we consider the indentity $\ln(x)=\lim_{c\rightarrow 0}(1/c)(x_c-1)$.

[8] P. Meakin, *Fractals, Scaling, and Growth Far from Equilibrium* (Cambridge University Press, Cambridge, 1998); J. Krim and G. Palasantzas // *Int. J. of Mod. Phys.* B**9** (1995) 599.

[9] A. –L. Barabási and H. E. Stanley, *Fractal Concepts in Surface Growth* (Cambridge University Press, Cambridge, 1995).

[10] G. Palasantzas, S. A. Koch and J. Th. M. De Hosson // *Appl. Phys. Lett.* **81** (2002) 1089.
[11] D. J. Eaglesham, A. E. White, L. C. Feldman, N. Moriya and D. C. Jacobson // *Phys. Rev. Lett.* **70** (1993) 1643.
[12] C. G. Zimmermann, M. Yeadon, K. Nordlund, J. M. Gibson, R. S. Averback, U. Herr and K. Samwer // *Phys. Rev. Lett.* **83** (1999) 1163.
[13] M. Kardar, G. Parisi and Y. C. Zhang // *Phys. Rev. Lett.* **56** (1986) 889; M. Forest and L. – H. Tang // *Phys. Rev. Lett.* **64** (1991) 1405.
[14] J-J. Aué and J. Th. M. De Hosson // *Appl. Phys. Lett.* **71** (1997) 1347.
[15] W. E. Wolf and J. Villain // *Europhys. Lett.* **13** (1990) 389.
[16] D. Kashchiev // *Surf. Sci.* **55** (1976) 477; B. Lewis // *Surf. Sci.* **21** (1970) 289.
[17] S. K. Sinha, E. B. Sirota, S. Garoff and H. B. Stanley // *Phys. Rev. B* **38** (1988) 2297.
[18] H. D. Bal and P. W. Schmidt // *Phys. Rev. Lett.* **53** (1984) 596.
[19] G. Palasantzas and J. Krim // *Phys. Rev. B* **48** (1993) 2873.
[20] C. Thompson, G. Palasantzas, Y.P. Feng, S. K.Sinha and J. Krim *// Phys. Rev. B* **49** (1994) 4902.
[21] J. Krug // *Adv. Phys.* **46** (1997) 139; K. Fang *et al.* // *Phys. Rev. B* **49** (1994) 8331; C. J. Lanczycki *et al.* // *Phys. Rev. B* **57** (1998) 13132; J. Krug // *Phys. Rev. Lett.* **75** (1995) 1795.